# Analytical and Numerical Investigations of Ring Resonators

Funda Akleman [†] Levent Sevgi [&]

*Abstract* **Rectangular vs. cylindrical finite-difference time-domain (FDTD) electromagnetic modeling is discussed, and characteristic tests and comparisons are presented depending on the analytical and numerical analysis of ring type circular resonators. A ring resonator is modeled with both rectangular- and cylindrical-FDTD packages which are also calibrated against analytical exact solution derived in terms of cylindrical Bessel functions. Applications of the periodic boundary condition in modeling circular (rectangular) structure via rectangular (circular) FDTD is also given.**

## 1 INTRODUCTION

In this study, modeling of cylindrical structures such as groove resonators [1], microstrip ring resonators [2] via rectangular and cylindrical representations of Finite Difference Time Domain (FDTD) method is considered. Any EM problem can be represented in a discrete environment within the FDTD computation volume either in rectangular or in cylindrical coordinates as long as the problem specific boundary and initial conditions are adequately modeled and stability/numerical dispersion conditions are satisfied.

A ring (circular) resonator with rectangular cross-section and non-penetrable (perfectly electrical conductor, PEC) walls (Fig.1) is a canonical structure for the comparisons of rectangular and cylindrical FDTD packages, since

i. Analytical exact (reference) solution can be derived in terms of Green's functions in cylindrical coordinate system,
ii. The structure fits into the cylindrical FDTD space without any staircase discretization error,
iii. The structure may be represented in the rectangular FDTD with staircase approximation (and introduces discretization errors)
iv. The structure may also be represented in the rectangular FDTD if periodic boundary condition (PBC) is applied at both terminations (without using staircase approach).

In this study, a ring resonator is modeled with both rectangular- and cylindrical-FDTD packages, which are also calibrated against analytical exact solution derived in terms of cylindrical Bessel functions. Applications of the periodic boundary condition in modeling of ring resonator via rectangular FDTD using rectangular cross-section waveguide are also given.

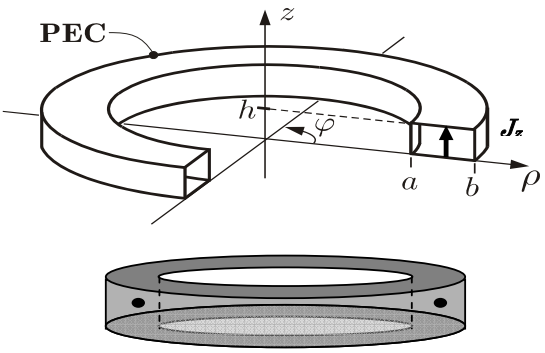


Figure 1: Rectangular cross section ring resonator

## 2 RING RESONATORS AND GREEN'S FUNCTION REPRESENTATIONS

The ring resonator as pictured in Fig. 1 is bounded between a and b radially $(a < \rho < b)$, between 0 and h vertically $(0 \le z \le h)$, and between 0 and $2\pi$ azimuthally $(0 \le \varphi \le 2\pi)$. The Green's function problem for a z-directed short dipole source at $(\rho', \varphi', z')$ inside the resonator can be obtained via the wave equation in the cylindrical coordinate system

$$\left[\frac{1}{\rho}\frac{\partial}{\partial\rho}\left(\rho\frac{\partial}{\partial\rho}\right)+\frac{1}{\rho^2}\frac{\partial^2}{\partial\varphi^2}+\frac{\partial^2}{\partial z^2}+k^2\right]G(\rho,\varphi,z;\rho',\varphi',z') = -\frac{\delta(\rho-\rho')\delta(\varphi-\varphi')\delta(z-z')}{\rho} \quad (1)$$

[†]Istanbul Technical University, Electronics and Communication Engineering Department, Maslak, 34469 Istanbul,Turkey
e-mail: akleman@itu.edu.tr, tel:+90 212 2853495
[&] Doğuş University, Electronics and Communication Engineering Department, Zeamet Sok. No. 21, Acıbadem 34722 Istanbul,Turkey
e-mail: lsevgi@itu.edu.tr, tel:+90 532 5995090

1-4244-0767-2/07/$20.00 ©2007 IEEE

together with the boundary conditions

$$\partial G/\partial z = 0 \text{ at } \quad z = 0, h \text{ and } \quad G = 0 \quad \text{at} \quad \rho = a, b \tag{1a}$$

and, periodicity condition in $\varphi$-direction. The width $w$ of the cross-section of the ring resonator is $w = b - a$ and the mean peripheral length is $L = \pi(b + a)$.

The wave equation (1) for the non-penetrable ring resonator can be reduced to three 1D wave equations (if the separation of variables technique is applied) and can be solved separately. Following this procedure yields the solution in terms of first and second kind Bessel functions as [3]

$$G(\rho,\varphi,z;\rho',\varphi',z') = \sum_{m=0}^{\infty} A_m \cos\left(\frac{m\pi}{h}z\right)\cos\left(\frac{m\pi}{h}z'\right) \frac{1}{2\pi}\sum_{n=-\infty}^{\infty} e^{jn(\varphi-\varphi')} \sum_{l=1}^{\infty} \frac{R(\lambda_{mnl}\rho)R(\lambda_{mnl}\rho')}{k^2-(m\pi/h)^2-\lambda_{mnl}^2} \tag{2}$$

where

$$A_m = \begin{cases} \dfrac{1}{h} & m = 0 \\ \dfrac{2}{h} & else \end{cases} \tag{2a}$$

$$R(\lambda\rho) = N\left[J_n(\lambda\rho) + C_1 Y_n(\lambda\rho)\right], \quad C_1 = \frac{J_n(\lambda a)}{Y_n(\lambda a)} \tag{2b}$$

$$J_n(\lambda b) + \frac{J_n(\lambda a)}{Y_n(\lambda a)} Y_n(\lambda b) = 0 \; at \; \lambda = \lambda_{mnl} \tag{2c}$$

and the normalization constant is found as

$$N = \frac{1}{\left[\int_a^b \left[R(\lambda_{mnl}\rho)\right]\rho d\rho\right]^{1/2}} \tag{2d}$$

.

Here, $J_n(\lambda\rho)$ and $Y_n(\lambda\rho)$ are the first and second kind Bessel functions, respectively. Equation (2) can be used to calculate field distribution at any point inside the ring resonator excited by the z-directed short dipole. The resonance frequencies can also easily be found via

$$f_{mnl} = \frac{c}{2\pi\sqrt{\varepsilon_r}}\sqrt{\left(\frac{m\pi}{h}\right)^2 + \lambda_{mnl}^2} \tag{3}$$

where $\varepsilon_r$ is the relative dielectric permittivity inside the resonator. Unfortunately, this requires a triple series summation with infinite number of terms, therefore one need to introduce simplifications in order to reduce the numerical burden. Also, a small loss should be introduced to the medium inside the resonator (i.e., k is assumed complex) in order to avoid numerical problems at frequencies close to the resonator's resonances. A z-directed line source with amplitude $I_0$ (see Fig. 2)

$$\vec{J}_z = -\vec{e}_z I_0 \frac{\delta(\rho-\rho')\delta(\varphi-\varphi')}{\rho} \tag{4}$$

further simplifies the solution (i.e., $\partial/\partial z \equiv 0$), and triple summation reduces to a double summation. In this case the resonance frequencies are obtained as

$$f_{0nl} = \frac{c}{2\pi\sqrt{\varepsilon_r}}\lambda_{0nl} \tag{5}$$

## 3 RING RESONATORS AND FDTD MODELING

In this study, three approaches are used for the analysis of ring resonators via FDTD and tested against each other as well as analytical exact solution. The modeling of any type of ring resonators (i.e groove, microstrip, etc.) via FDTD in both Cartesian and cylindrical coordinates is straightforward. In general, it may be extremely time consuming to work with cylindrical FDTD simulations in the vicinity of the origin ($\rho \to 0$) since the cell size in $\varphi$-direction decreases with decreasing $\rho$, and this requires very small time steps (in order to satisfy Courant stability criterion). This difficulty is removed if the origin is excluded (as in the ring resonator), or if (no variation in $\varphi$-direction), for example, as in body of revolution (BOR) type radiation problems.

It is also possible to model a ring resonator by applying periodic boundary condition (PBC) at the both ports of a regular waveguide in Cartesian coordinates to simulate the angular periodicity (Fig. 2). In this study, the ring resonator given in Fig. 1 is analyzed using rectangular cross section waveguide with the help of "wrap-around" approach required to apply PBC [4].

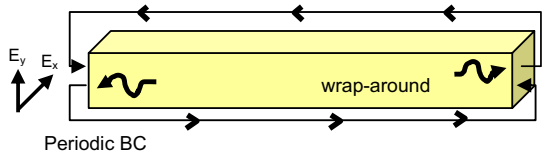


Figure 2: Rectangular cross section waveguide with PBC applied at input and output ports

## 4 NUMERICAL APPLICATIONS

In this study, three FDTD packages are prepared; R-FDTD based on FDTD in rectangular (Cartesian) coordinates, C-FDTD based on FDTD in cylindrical coordinates and P-FDTD based on rectangular FDTD together with PBC in longitudinal direction. The rectangular system is usually preferred because the spatial cell sizes are uniform over the whole R-FDTD space, while in C-FDTD one side of the cell is $\rho\Delta\varphi$, which varies in radial direction. This should be taken into account when the FDTD parameters are specified.

The validation and verification the results obtained via these FDTD packages are realized by comparing them with the analytical exact solution. A circular ring resonator with non-penetrable PEC walls is taken into consideration with the parameters $a = 6\,\text{mm}$, $b = 12\,\text{mm}$ and $h = 10\,\text{mm}$. The resonator is excited with a z-directed and sine-modulated Gaussian short pulse line source at $\rho' = (a+b)/2$ and $\varphi' = 0$, of which center frequency is 25GHz and bandwidth is 10GHz. The cell sizes for C-FDTD and R-FDTD are taken as $\Delta z = \Delta\rho = 0.2\,\text{mm}, \Delta\varphi = 1^\circ$ and $\Delta x = \Delta y = \Delta z = 0.2\,\text{mm}$, respectively as the first test case. In R-FDTD number of cells required to model cylindrical objects is greater, therefore computation time is longer compared to the C-FDTD for the same number of time steps. Here 10000 time steps is used for the first scenario and $E_z$ is accumulated at an observation point of $\varphi = 120^\circ$ $\rho = (a+b)/2$ and $z = h/2$ for both packages. The resonance frequencies are obtained by applying off-line DFT (discrete Fourier transform) to the time accumulation of $E_z$ for both packages and the results are plotted in Fig. 3 together with the analytical exact results. In Fig. 3, solid line, dashed line and symbols correspond to resonance frequencies obtained via R-FDTD, C-FDTD and analytic solution, respectively. Since the chosen bandwidth does not include resonances corresponding to higher order roots of (2c), only $l = 1$, the first root of (2c), is taken into consideration for the analytical results. Besides, (5) is used to calculate the resonance frequencies since $m = 0$ (i.e., line source in z-axis), therefore in Fig. 3 the resonance frequencies 24.85GHz, 25.43GHz, 27.11GHz, 29.67GHz, 32.89GHZ, correspond to $n = 0,1,2,3,4$ with $l = 1$ and $m = 0$, respectively. Although a good agreement between the numerical and analytical results is observed in Fig. 3, there is a slight difference between R-FDTD and C-FDTD because of the staircase approximation in R-FDTD. This deviation can be reduced if finer cell size (i.e. $\Delta x = \Delta y = \Delta z = 0.1\text{mm}$) is used in RFDTD. The resonance frequencies obtained via R-FDTD with fine discretization is given in Fig. 4 together with C-FDTD and analytical results to emphasize the effect of staircase approach in R-FDTD.

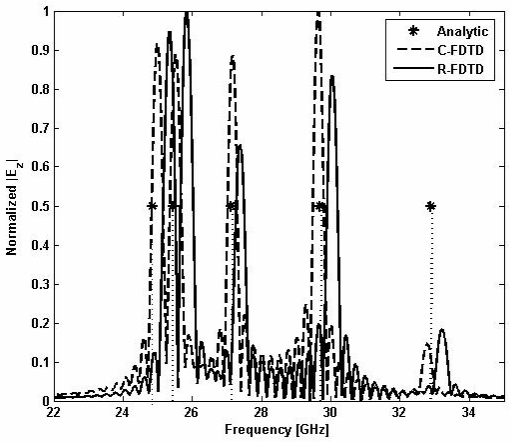


Figure 3: Resonance frequencies obtained via C-FDTD (dashed), R-FDTD with coarse grid (solid) and analytic solution (symbol)

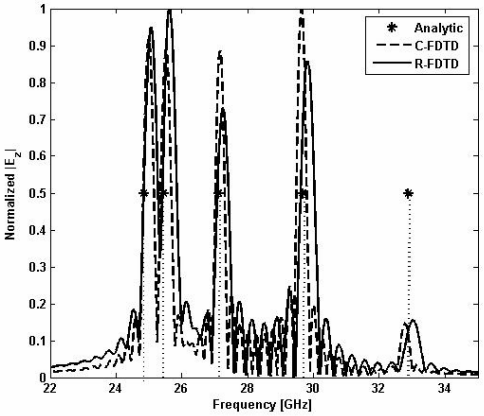


Figure 4: Resonance frequencies obtained via C-FDTD (dashed), R-FDTD with fine grid (solid) and analytic solution (symbol)

FDTD with PBC (P-FDTD) is also applied to a rectangular cross-section waveguide (see Fig. 2) to

obtain the resonance frequencies instead of regular R-FDTD or C-FDTD as it is explained in Section 3. In this case, the longitudinal length of the waveguide is chosen to be equal to the mean peripheral of the circular ring resonator, $L = \pi(a+b)$. When PBC is applied at the input and output ports of the rectangular cross-section waveguide, the azimuthal periodicity of the circular ring resonator is achieved. The width and height of the rectangular cross-section waveguide is taken as $w = (b-a)$ and equal to the height $h$ of the ring resonator, respectively. The resonance frequencies obtained via P-FDTD are plotted in Fig. 5 together with the data calculated by C-FDTD and analytical solution. As it is observed, there is a good agreement between the results.

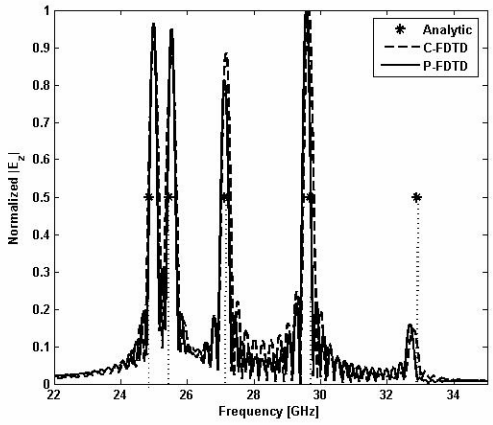


Figure 5: Resonance frequencies obtained via C-FDTD (dashed), P-FDTD (solid) and analytic solution (symbol)

## 5 CONCLUSIONS

In this study, rectangular vs. cylindrical finite-difference time-domain (FDTD) electromagnetic modeling is discussed, and characteristic tests and comparisons are presented depending on the analytical and numerical analysis of ring type circular resonators. Both rectangular and cylindrical FDTD codes are prepared for this purpose. Characteristic tests are performed on the canonical ring (circular) type resonator, and the packages are validated against analytical exact solutions derived for both rectangular and cylindrical coordinates. It has been also shown, using the 3D-FDTD method, that the resonance frequencies of a ring resonator can also be obtained using PBC and wrap-around technique at the input and output ports of a finite-length rectangular waveguide.

## References


[1] S. Aydınlık Bechteler, L. Sevgi, "Millimeter Waveband Semi-symmetrical Groove Guide Resonator", IEEE Microwave Magazine, Vol. 5, No. 3, pp.51-61, Sep 2004

[2] E. Semouchkina, W. Cao, M. Lanagan, R. Mittra, W. Yu "Combining FDTD simulations with measurements of microstrip ring resonators for characterization of low- and high-K dielectrics at microwaves", Microwave and Optical Technology Letters, 29,121-24,2001

[3] A. Ishimaru, Electromagnetic Wave Propagation, Radiation and Scattering, Prentice Hall, 1991

[4] P. Harms, R. Mittra, W. Ko, "Implementation of the periodic boundary condition in the finite-difference time-domain algorithm for FSS structures," *IEEE Trans. Antennas Propagat.,* vol. 42, no. , Sept. 1994, pp. 1317–1324